The Effect of the Dielectric Environment on Electron Transfer Reactions at the Interfaces of Molecular Sensitized Semiconductors in Electrolytes

Davide Moia,[1,2,*] Masato Abe,[1] Pawel Wagner,[3] Hiromu Saguchi,[1] Nagatoshi Koumura,[4] Jenny Nelson,[2] Piers R.F. Barnes,[2,*] Shogo Mori[1,*]

[1] Division of Chemistry and Materials, Faculty of Textile Science and Technology, Shinshu University, 3-15-1 Tokida, Ueda, Nagano 386-8567

[2] Department of Physics, Imperial College London, Prince Consort Road, SW7 2AZ, London

[3] ARC Centre of Excellence for Electromaterials Science, Intelligent Polymer Research Institute, University of Wollongong, Wollongong, NSW 2522, Australia.

[4] National Institute of Advanced Industrial Science and Technology, Interdisciplinary Research Center for Catalytic Chemistry, 1-1-1 Higashi, Tsukuba 305-8565, Japan.

*d.moia@fkf.mpg.de; piers.barnes@imperial.ac.uk; shogmori@shinshu-u.ac.jp

Abstract

Electron transfer theories predict that rates of charge transfer vary with the dielectric properties of the environment where the reaction occurs. An appropriate description of this relation for molecular sensitized semiconductors in electrolytes must account for the restricted geometry of these systems compared to 'free' molecules in solution. Here, we explore the extent to which dielectric properties of the surrounding medium can explain the rates of charge transfer processes, measured using transient absorption spectroscopy, involving photo-oxidized thiophene-carbazole based molecules on oxide semiconductors in inert or redox-active electrolytes. We observe no clear correlation between the activation energy of hole hopping between molecules on oxide surfaces or the recombination rate between photogenerated electrons in the oxide and holes on the adsorbed molecules and the dielectric properties of the surrounding solvent. The activation energy of hole hopping tends to increase with time following initial photo-generation of the holes, which we attribute to energetic disorder in the molecular monolayer. The recombination rate in different solvents scales with the hole hopping rate. It can also be varied by adding inert salts in the electrolyte and by controlling the access of cations in solution to the oxide surface. Finally we show that fast electron transfer from cobalt complexes to photo-oxidized molecules in solvents with low polarity is verified, but the kinetics are limited by the ionic dissociation. Our study highlights the importance of electronic coupling between the redox active components and their solvation, beside the reorganization energy and the driving force, in the determination of electron transfer rates at molecular sensitized interfaces in electrolytes.

Introduction

Electron transfer is the most fundamental reaction in all natural (photo)electrochemical systems that include redox active molecules and underlies the working mechanism of all electronic and electrochemical devices. For example, in a dye sensitized solar cell (DSSC) a mesoporous oxide semiconducting film sensitized with light absorbing dye molecules and an electrolyte containing a redox couple are combined to convert light into electrochemical energy.[1] This conversion relies on a sequence of processes that include light absorption by the dyes, charge separation at the oxide/dye/electrolyte interfaces and charge transport to the electrodes of the cell.[2] Understanding and controlling the factors influencing electron transfer processes is therefore of utmost importance to improve the performance of these devices.

The most successful and widely used theory to date that describes electron transfer processes between weakly coupled redox sites is non-adiabatic Marcus theory. The rate of electron transfer between an electron donor and an electron acceptor can be expressed, according to this theory, as follows:

$$\Gamma = \frac{2\pi}{\hbar}\frac{|J|^2}{\sqrt{4\pi\lambda k_B T}} e^{-\frac{(\Delta G_0+\lambda)^2}{4\lambda k_B T}}. \qquad \text{Eq.1}$$

In equation 1, the rate Γ is a function of three main parameters. The electronic coupling J is related to the electron wavefunction overlap between the two redox sites. The driving force of the electron transfer reaction ΔG_0 is the difference in free energy between the products (after electron transfer has occurred) and the reactants (before electron transfer has occurred). Finally, the reorganization energy λ represents a measure of the energy involved in structural reorganization of the donor and acceptor as well as of the environment, upon electron transfer. The parameters T, k_B and $\hbar$ correspond to temperature, Boltzmann's constant and Planck's constant. The equation refers to donor acceptor systems in an environment approximated as an isotropic dielectric continuum.

Marcus theory has been invoked to investigate all electron transfer processes occurring in a DSSC. The processes that specifically involve a photo-oxidized dye are shown in Figure 1a and are: (i) the hole hopping between dyes anchored to the oxide surface; (ii) the recombination of a hole on a dye with an electron in the oxide particle; (iii) the dye regeneration by a redox-couple. Prior to these processes, photoinduced electron injection is another important electron transfer process at this interface. Electron injection has been characterized in detail in previous literature.[3,4]

The hole hopping process occurs between nominally identical redox-sites. Consequently, to a first approximation, $\Delta G_0 = 0$ and the process can be defined as a self-exchange reaction. We and other groups have recently correlated hole hopping between dyes to the regeneration and collection efficiency of solid state DSSCs,[5,6,7] and to the oxidized dye lifetime of dye sensitized TiO_2 in inert electrolytes.[8,9] The potential of hole hopping for catalysis applications has also been discussed in the literature.[10,11,12] Despite not being widely invoked as an important mechanism, these reports suggest

that hole hopping between adsorbed molecules has a critical influence on the charge transfer dynamics of device interfaces and consequently the device performance.

Recombination between electrons in the metal oxide and holes in adsorbed molecules has been described in terms of electron transport limitation in the metal oxide. Electron trapping-detrapping processes occurring for the case of nano-sized semiconductor particles result in a dispersive decay of the electron hole population (i.e. recombination occurring throughout a broad range of time scales).[13] Reaction limited recombination has also been reported.[14] Interestingly, some systems showed a decrease in the reaction rate upon increasing the driving force while other systems showed the opposite behavior.[15,16,17] According to Marcus theory, these observations would correspond to the case of $\Delta G_0 + \lambda < 0$, known as Marcus inverted region (see dash line in Figure 1b), and $\Delta G_0 + \lambda > 0$ known as Marcus normal region (solid line in Figure 1b), respectively.

The dye regeneration process involves electron transfer from a redox couple (electron donor) to a photo-oxidized dye (electron acceptor), and its driving force is in general non-zero. A common observation is that increasing the driving force of this process increases its rate, consistent with Marcus theory under the conditions of $\Delta G_0 + \lambda > 0$.[18,19,20] In terms of device performance, fast regeneration is beneficial to the charge separation efficiency. However, increasing the driving force increases the energy loss involved in the regeneration process, adversely affecting the open circuit voltage in a solar cell. Finding strategies that can increase the regeneration rate with minimal values of the driving force is therefore a priority in the field of DSSCs.[21]

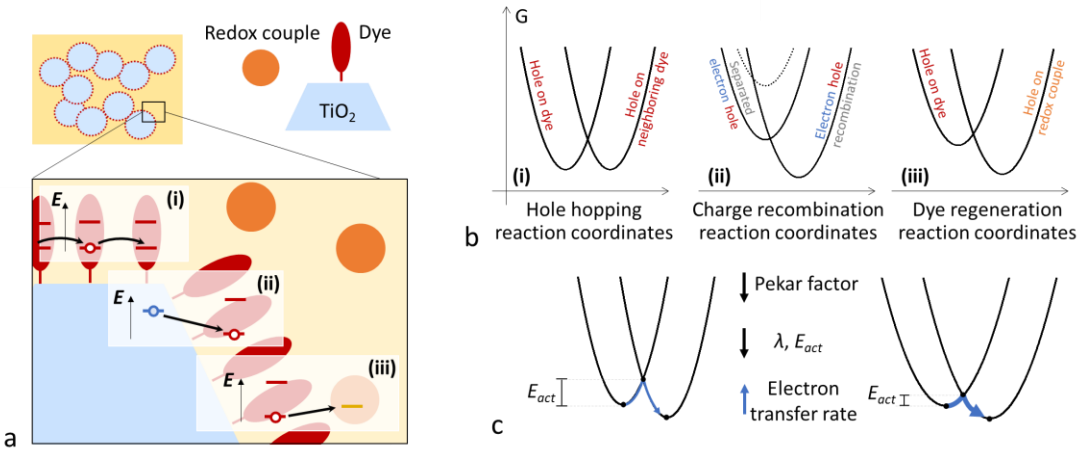


Figure 1. (a) Structure of a dye sensitized solar cell including a dye sensitized titanium dioxide mesoporous film and an electrolyte containing a redox-couple. The schematics, (i), (ii) and (iii) illustrate the processes of hole hopping between dyes, recombination of electrons in the oxide with holes on adsorbed dyes, and dye regeneration by a redox-couple. (b) Diagram of the free energy of reactants and products as a function of one reaction coordinate for a self-exchange reaction (i) and for an electron transfer reaction between a donor and an acceptor

involving a negative free energy change (ii, iii). (c) Expected variation in free energy and electron transfer rate upon variation in Pekar factor of the solvent for the case of $\Delta G_0 + \lambda > 0$ according to non-adiabatic Marcus theory (the change in electron transfer rate is expected to be opposite for $\Delta G_0 + \lambda < 0$).

Equation 1 indicates that Γ increases when decreasing λ for $\Delta G_0 + \lambda > 0$, while it decreases when $\Delta G_0 + \lambda < 0$. The reorganization energy of charge transfer λ can be separated into the sum of an inner sphere component λ_i, which is the energy involved in the structural reorganization of the redox sites upon charge transfer, and an outer sphere component λ_o, that accounts for the solvent's reorganization. λ_i can be varied by changing the chemical structure of the redox-sites. According to Marcus theory, λ_o is inversely proportional to the size of the donor and acceptor units involved in the reaction and increases for longer distance between the two units.[22] It is also proportional to the Pekar factor which is defined as $\varepsilon_{eff}^{-1} = \varepsilon_{opt}^{-1} - \varepsilon_s^{-1}$, where ε_{opt} and ε_s are the optical and static dielectric constants of the surrounding environment. Assuming spherical reactants with radii a_1 and a_2, at a center to center distance of R, and a single electron transfer (of charge q), λ_o can be expressed as:

$$\lambda_0 = \frac{q^2}{4\pi\epsilon_0}\left(\frac{1}{2a_1} + \frac{1}{2a_2} - \frac{1}{R}\right)\epsilon_{eff}^{-1} \quad , \qquad \text{Eq. 2}$$

where ϵ_0 is the dielectric permittivity of vacuum. Note that models based on more relevant geometries than the simplified spherical case have also been considered.[23,24] These still highlight the importance of the parameter ε_{eff}^{-1} for the determination of λ_o. In a previous study, we estimated the reorganization energy of hole hopping between dyes in 0.1 M tetrabutylammonium perchlorate (TBAP) in acetonitrile from temperature dependent cyclic voltammetry measurements. Comparison between these values with calculations suggested that the dominant contribution to the overall value of λ is from λ_o when polar solvents are used.[25,26]

When considering the same dye, using solvents with different dielectric properties is expected to yield differences in λ_o and hence electron transfer rate according to equation 1. However, previous electrochemical studies of hole and electron hopping in dye sensitized mesoporous oxide films in different solvents by the Grätzel group reported limited or opposite dependence of the charge transfer rate on the dielectric constant of the solvent to that expected theoretically.[27,28] Electrochemical approaches however rely on the use of electrolytes that contain inert salts, which affect the dielectric constant of the environment.[26,29] Transient absorption anisotropy has been shown as a technique to monitor the rate of hole hopping and that can be applied to dye sensitized films immersed in solvents that need not contain any ions enabling better control of the dielectric environment.[10] Using this technique, considering dye sensitized samples in solvents without inert salts, we have shown that an opposite trend compared to what predicted by Marcus theory can be observed, where increasing the electrolyte's Pekar factor resulted in faster hole hopping.[8] Similar results have also been shown in a

spectroscopic study of hole hopping in a c-shape molecule containing donor and acceptor moieties, where the observed fast hole hopping in high polarity solvents was explained in terms of the change in packing and coupling between donor and acceptor moieties upon increase of the solvent dielectric constant.[30]

Based on this literature, Equation 1 seems to have limited applicability to explain the reactions occurring in molecular sensitized oxide semiconductors in electrolytes. In these systems, the molecules are anchored on the oxide and the distance between donor and acceptor is rather fixed. This, on the one hand, could simplify the analysis due to the lesser degrees of freedom involved, on the other hand it is expected to complicate the relation between solvent Pekar factor and reorganization energy from the case of free molecules in solution, with also possible repercussions on the electronic coupling of electron transfer reactions. On a practical level, the questions are: to what extent do the dielectric properties of the solvent and oxide control the rates of electron transfer at oxide/dye/electrolyte interfaces? What other parameters are relevant to these systems, besides reorganization energy, driving force and electronic coupling of electron transfer? Here, we address these questions by probing the rate of reactions (i), (ii) and (iii) using transient absorption and transient absorption anisotropy spectroscopy while varying the experimental parameters that are expected to determine the screening and the electrostatic properties at the interfaces in molecular sensitized oxides in inert and redox active electrolytes. We chose oxide materials, and electrolyte solvents that cover a broad range of Pekar factor values and varied the electrolyte composition in terms of redox couple, inert ions and additives. Finally we propose an explanation for the discrepancies between the observed trends and the existing theoretical framework, highlighting the role of disorder in the dye monolayer, of the relationship between the different reactions and of electrostatic and solvation effects at the oxide/dye/electrolyte interface.

Experimental method

Sample preparation: dyed porous metal oxide films were prepared with common procedures (see section 1 of the Supporting Information). The MK2 dye and other thiophene based dyes were used, given their proven photo-stability.[31] MK2 was purchased from Aldrich. MK3, MK75 and MK147 were also considered.[32,33] The structures of the MK2 and MK147 dyes, and the electrolyte components used here are shown in Figure 2. MK3 and MK75 have a similar structure to MK2, with three thiophenes without alkyl chains and two thiophenes with alkyl chains respectively. Synthesis of the MK147 dye is presented in section 2 of the Supporting Information. Cobalt redox couples were chosen in that they are a one electron single step regenerative system. The complexes $Co^{(II)}(bpy)_3[B(CN)_4]_2$ and $Co^{(III)}(bpy)_3[B(CN)_4]_3$ were used in the study of the effect of inert salts on the regeneration kinetics. The complexes $Co^{(II)}(bpy)_3[TFSI]_2$ and $Co^{(III)}(bpy)_3[TFSI]_3$ were used for the investigation of the solvent dependence given their higher solubility in low polarity solvents. In all

experiments, both $Co^{(II)}$ and $Co^{(III)}$ complexes were added in the electrolytes at a constant ratio of $[Co^{(II)}]/[Co^{(III)}] = 11.1$. In the text we specify the experimental conditions referring to the concentration of $Co^{(II)}$ species only for brevity. The structure of the dye molecules, the redox couple, the salts, the additive and the solvents used in this work are shown in Figure 2. The samples were fabricated using electrolytes based on solvents with different dielectric properties. The static dielectric constant, refractive index and Pekar factor of each solvent are listed in Table 1. The preparation of the samples was done in ambient conditions. The presence of water on the surface of TiO_2 may also contribute to the effective dielectric environment. Apart from the anchoring group, the dyes' chemical structure has a hydrophobic character. We therefore expect the dyes to interact to a limited extent with water molecules, and rather to be solvated by the organic solvents used in the study.

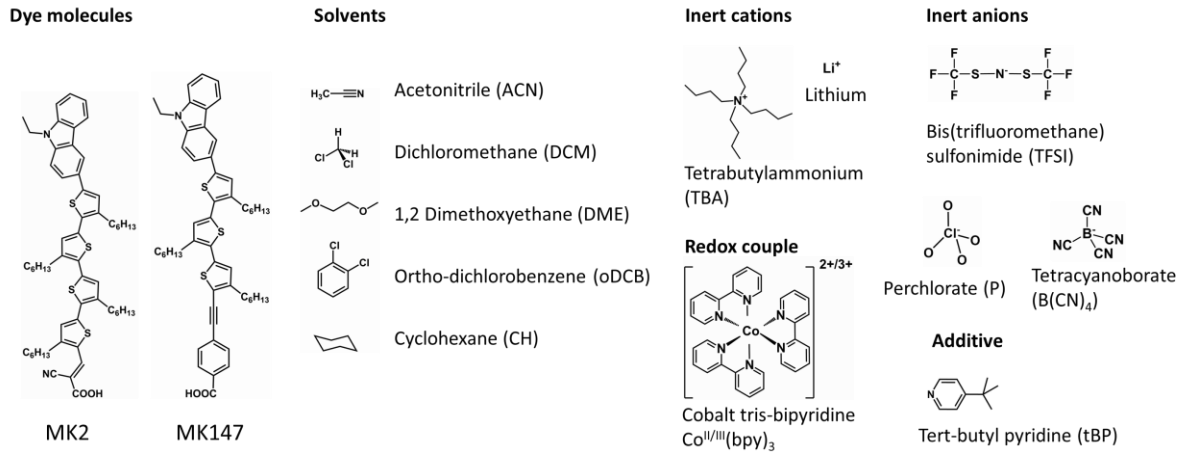


Figure 2. Chemical structure of the materials used in this study.

Table 1. Dielectric properties of the solvents used in this study. Dielectric constants were taken from reference [34] and refer to data in the temperature range between 293 and 298 K. Refractive index data were taken from reference [35] for 298 K. The Pekar factor was calculated as $\epsilon_{eff}^{-1} = n^{-2} - \epsilon_s^{-1}$.

Solvent	**Static dielectric constant ε_s**	**Refractive index n (at 589.3 nm)**	**Pekar factor ε_{eff}^{-1}**
Acetonitrile (ACN)	36.6	1.342	**0.53**
Dichloromethane (DCM)	8.93	1.421	**0.38**
1,2-Dimethoxyethane (DME)	7.30	1.377	**0.39**
Ortho-dichlorobenzene (oDCB)	10.1	1.550	**0.32**
Cyclohexane (CH)	2.02	1.423	**0.00**

Transient absorption and transient absorption anisotropy measurements: the samples were placed in the setup such that the probe light (red laser 780 nm, CUBE, Coherent) passed through the active area, and the pump (532 nm Nd:YAG pulsed laser, INDY, Spectra Physics) illuminated an area that was larger than the active area of the sample. For temperature dependent measurements, a cryostat (CoolSpek, UNISOKU) was used to cover the temperature range between 318 K and 243 K. This range was chosen, and adapted depending on the solvent, to avoid evaporation or freezing of the solvents used. The pump laser intensity was set between 10 and 15 μJ cm^{-2} per pulse. A repetition rate of 10 Hz was used for the hole hopping study, 1 Hz for the recombination study and 5 Hz for the dye regeneration study, unless stated otherwise. The 780 nm laser beam was polarized before passing through the sample at the magic angle (54.7°) with respect to the (vertical) polarization of the pump for transient absorption measurements, or at 0° and 90° for anisotropy measurements.[36] The beam was focused on to a photodetector after passing through the sample through a series of lenses and without any mirror. The change in transmission was detected through the photodetector, amplified, and collected using an oscilloscope. The optical density data were calculated from the time resolved change in transmission $\Delta T(t)$ and the background transmission T using the relation $\Delta \mathrm{OD}(t) = -\Delta T(t)/(2.3T)$.

The transient absorption anisotropy r_{exp} of dye sensitized oxide mesoporous films was calculated as in previous reports using the formula:

$$r_{exp}(t) = \frac{\Delta \mathrm{OD_V}(t) - \Delta \mathrm{OD_H}(t)}{\Delta \mathrm{OD_V}(t) + 2\Delta \mathrm{OD_H}(t)} \qquad \text{Eq.3}$$

Where $\Delta \mathrm{OD_V}(t)$ and $\Delta \mathrm{OD_H}(t)$ are the transient absorption measurements performed with vertical and horizontal polarization of the probe beam.

Analysis of activation energy of hole hopping: The temperature dependent anisotropy data were analyzed as follows. The $\Delta \mathrm{OD_V}(t)$ and $\Delta \mathrm{OD_H}(t)$ traces were smoothened using a moving average in log(t), where each value of r_{exp} at time $\bar{t}$ was calculated from the averaged values of $\Delta \mathrm{OD_V}(t)$ and $\Delta \mathrm{OD_H}(t)$ between the times $\bar{t}$/1.05 and $\bar{t}$ ×1.05. As shown in the results section, in the presence of disorder, the rate of hole transport following initial generation (at t = 0) decreases as holes hop to lower, more stable, energy states on average (other sources of variations in hopping rate include configurational disorder). Consequently, when evaluating the anisotropy decay, it is useful to determine effective hopping rates corresponding to the 'distance' already hopped, where the drop in $r_{exp}(t)$ can be used as proxy for the mean distance travelled. We achieve this by determining t_r which corresponds to the time at which an anisotropy decay reached the value $r = r_{exp}(t_r)$. The following formula was used:

$$\log_{10}[t_r] = \frac{\sum_{t=t_{min}}^{t_{max}} \log_{10} t \exp\left[-\frac{\left(r-r_{exp(t)}\right)^2}{2\sigma^2}\right]}{\sum_{t=t_{min}}^{t_{max}} \exp\left[-\frac{\left(r-r_{exp(t)}\right)^2}{2\sigma^2}\right]} \qquad \text{Eq. 4}$$

where σ is the estimated noise in the measurement and t_{min}, t_{max} determine the time range of the data considered. This formula assumes that noise following a Gaussian distribution affects the anisotropy trace. The value of σ is estimated by considering the root mean squared error between the anisotropy decay and a line fitted to the decay in logarithmic time within the ranges 10-20 μs and 100-200 μs. Typical values of σ between 0.003 and 0.006 were obtained. The time resolution of the experiment limits the maximum value of *r* considered in the data analysis for each sample, and therefore the minimum value of %*r* decay at which we present activation energy data in the Results section. We discuss additional notes on this and other aspects of the technique in section 3 of the Supporting Information.

Monte Carlo simulations: the simulations were run using the code described in reference[8] and are described in Section 4 of the Supporting Information.

Results

(i) Hole hopping between dyes

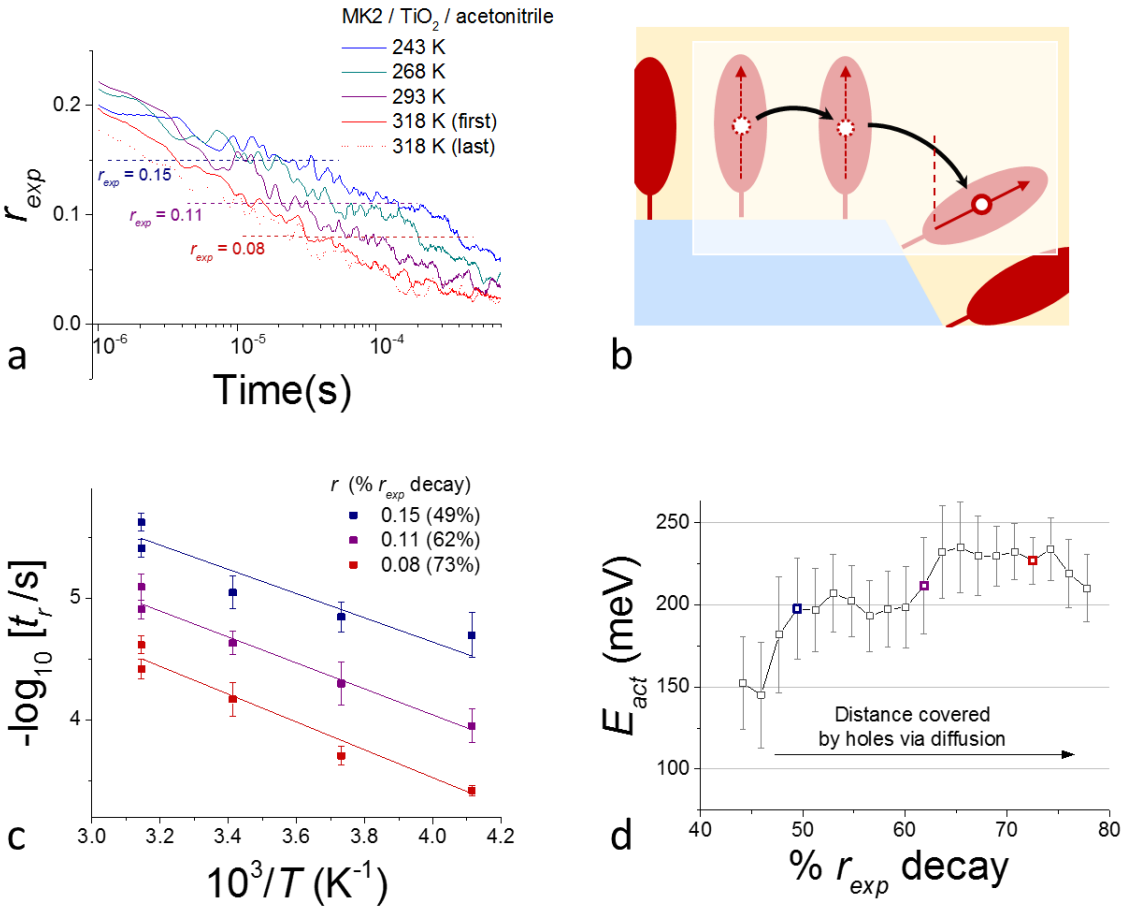


Figure 3. Measurement of activation energy for hole hopping between MK2 dyes sensitizing a TiO_2 mesoporous film in acetonitrile. (a) Temperature dependent transient absorption anisotropy measurements. (b) Interpretation of anisotropy decay in terms of holes migrating on the surface of the oxide particle, causing changes in orientation of the probed oxidized dye's transition dipole moment. (c) Arrhenius plot showing the rate (t_r^{-1}) corresponding to holes reaching a specific value of the anisotropy r as a function of temperature. (d) Values of activation energy extracted from the Arrhenius analysis of the data and plotted as a function of the fractional decay in anisotropy, assuming an initial value of $r_{exp} = 0.3$.

In Figure 3a, we show the results of the temperature dependent transient absorption anisotropy measurements performed on a MK2 sensitized TiO_2 mesoporous film immersed in acetonitrile. The protocol for the measurement is described in the experimental section and in section 5 of the Supporting Information. Decrease in temperature resulted in the slowing down of the anisotropy decay, consistent with a temperature activated process. Figure 3c displays an Arrhenius plot of the parameter t_r describing the kinetics of the decay. t_r is defined as the time at which a certain value of anisotropy r is reached after the laser pulse. The figure shows datasets corresponding to three selected values of anisotropy (also indicated in Figure 3a).

Fitting the Arrhenius relationship $(t_r)^{-1} = \exp(-E_{act}/k_BT)$ to the t_r *vs* T datasets for different values of r yielded the activation energies E_{act} illustrated in Figure 3d. These are plotted against the fractional change in anisotropy assuming an initial anisotropy value upon electron injection and structural relaxation of 0.3 (see discussion in section 6 of the SI). Note that since a monotonic decrease in anisotropy was observed for all the traces, the x-axis of Figure 3d is representative of the distance travelled by the holes via diffusion and of time passing after the laser pulse. The analysis shows that the value of E_{act} is not constant, instead a slight increase with time was observed in the range of 150 to 230 meV.

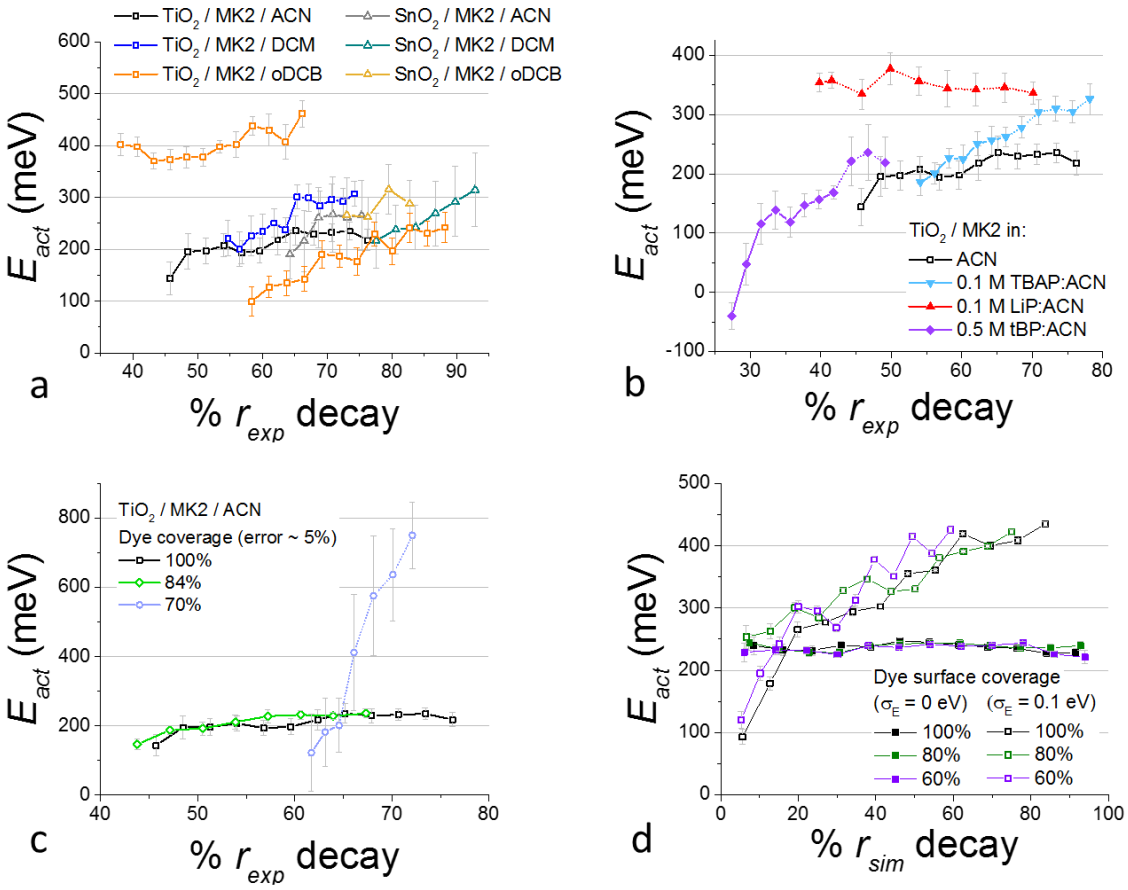


Figure 4. Activation energies as a function of anisotropy decay for hole hopping in MK2 sensitized films in different dielectric environments. (a) Effects of the mesoporous substrate (TiO_2, SnO_2) and of the solvent (acetonitrile, dichloromethane or ortho-dichlorobenzene). For the TiO_2 oDCB sample, the highest and lowest E_{act} datasets obtained are displayed to show the variations observed for this sample, as also commented in the text. (b) Effects of adding 0.1 M TBAP, 0.1 M LiP or 0.5 M tBP to acetonitrile electrolytes and (c) of the dye coverage. In all panels, datapoints joined by solid or dashed lines represent the results from fits using 4 or less than 4 temperatures respectively. (d) Simulated activation energy considering hole diffusion on the surface of a cubic particle, using values of 1 eV and 10 meV for the reorganization energy of hole transfer and electronic coupling between dyes respectively, and

for different conditions of dye surface coverage and energetic disorder (σ_E is the standard deviation of the Gaussian distribution of the HOMO energy levels involved in the hole hopping).

MK2 sensitized samples were then measured with the combinations of two different mesoporous oxides and three solvents having different dielectric properties. We also considered the effect of introducing the inert salt tetrabutyleammonium perchlorate (TBAP), lithium perchlorate (LiP) and the additive tert-butyl pyridine (tBP) in the electrolyte.

Figure 4a shows that relatively similar behaviour was obtained for most of the conditions considered here. In other words, no correlation was observed between the E_{act} values and the dielectric properties of the environment. We detect an increasing activation energy with fractional change in anisotropy for all systems and values in the order of 250 meV and 300 meV at high $\%r_{exp}$ decay (that is after the holes have diffused far enough from the photogeneration site). Samples using MK2 sensitized TiO_2 in ortho-dichlorobenzene showed limited reproducibility. In Figure 4a we show measurements of the two samples resulting in the highest and lowest values of E_{act}. In section 7 of the Supporting Information we show the full reproducibility study for this solvent and compare it to samples in acetonitrile. In the same section, transient absorption anisotropy measurements used to obtain the data under the conditions in Figure 4 as well as under additional conditions are shown. We observed a slight desorption of dyes from the surface of TiO_2 when immersing the sample in dichloromethane. In order to check the effect of this desorption on the measurement of activation energy, Figure 4c shows the measurement for a sample in acetonitrile which was immersed in dichloromethane solvent for about 10 minutes prior to the cell assembly and compare it with the data of the sample in acetonitrile shown in Figure 4a. The two profiles of activation energy are the same within error, suggesting that the desorption caused by dichloromethane, resulting in about 84% surface coverage, gives a negligible change in the hole transport performance of the sample. In the same figure, we also show the case of a sample that was dyed for a shorter time, resulting in (potentially non-uniform) lower average coverage of about 70%. This sample showed a significantly different behaviour, with a very steep increase in the apparent activation energy.

Figure 4d shows the activation energy extracted from Monte Carlo simulations of temperature dependent transient absorption anisotropy performed following the procedure described in reference[8] and in the section 4 of the Supporting Information, for different values of dye surface coverage and energetic disorder. The results show that the expected activation energy for a disorder free system is constant as a function of time, regardless of the dye surface coverage. Note that in this model, incomplete coverage is a source of static disorder which, however, does not introduce a temperature dependence. When we introduce a Gaussian energetic disorder in the value of the dyes' HOMO with standard deviation σ_E = 0.1 eV, a higher and delay-time dependent activation energy is obtained (all

the simulated anisotropy traces are displayed in Figure S5 of the Supporting Information). A small dependence on coverage is observed in this case too. Such dependence is expected to be more pronounced once the dye coverage approaches the percolation threshold. We note that, while energetic disorder is a plausible cause for the time dependent activation energy observed here, the trend displayed in Figure 4c might be related to additional effects occurring at low dye coverage, such as dynamic disorder in the form of fluctuation in dye orientation.[37]

(ii) Electron hole recombination in dye sensitized films immersed in inert electrolytes

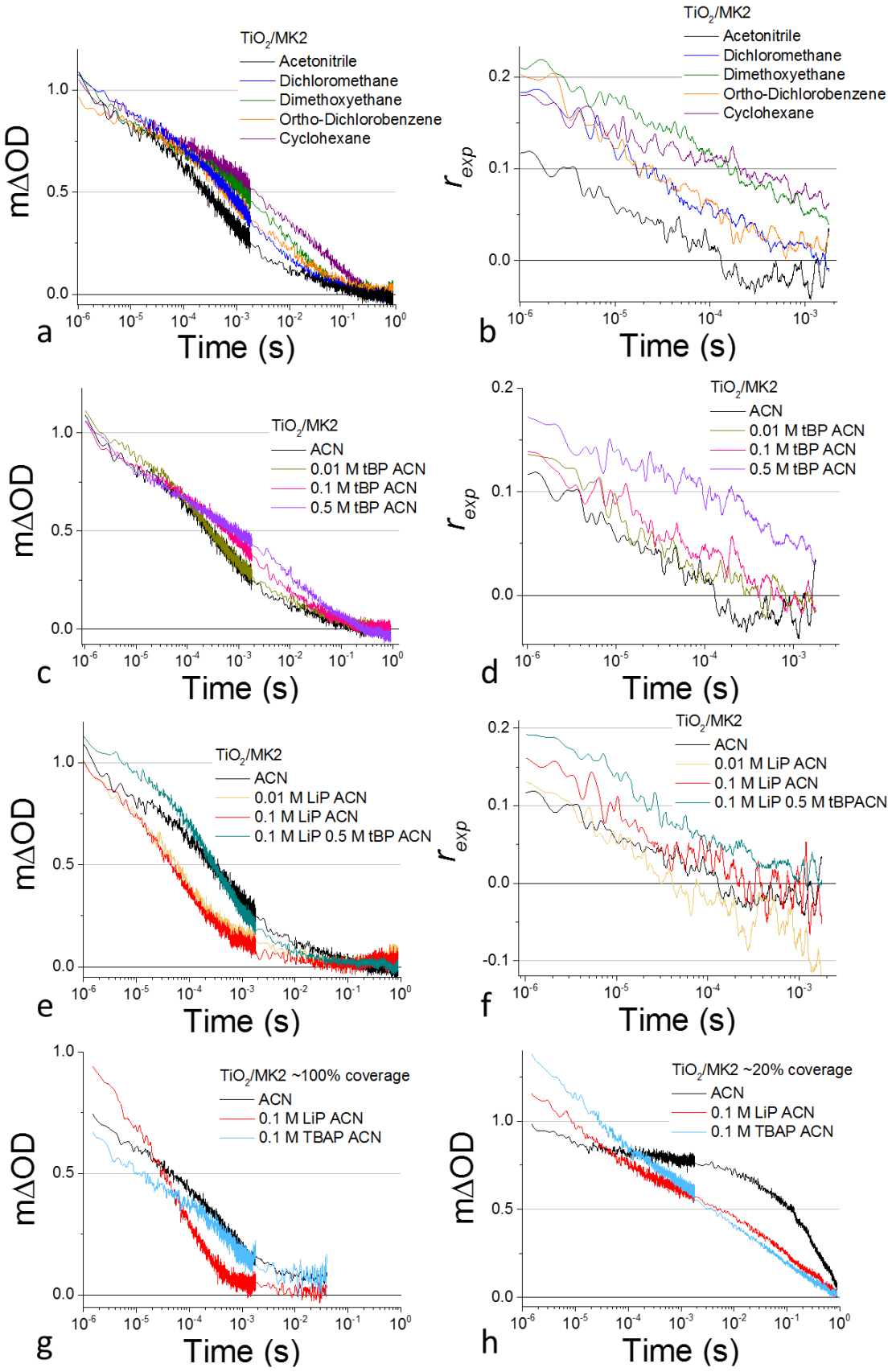


Figure 5 Transient absorption and transient absorption anisotropy measurements of MK2 sensitized TiO_2 mesoporous films showing the effect of: (a, b) different inert solvents; (c, d) addition of

tert-butyl pyridine in the solvent; (e, f) addition of lithium salt in the solvent. (g) and (h) show the effect of lithium perchlorate (LiP) and tetrabutylammonium perchlorate (TBAP) on the electron-hole recombination rate for the case of high and low dye coverage of the TiO_2 surface.

We then considered the recombination reaction between electrons in the oxide semiconductor and holes on adsorbed dyes. Figure 5a shows transient absorption spectroscopy measurements for MK2 sensitized TiO_2 mesoporous films immersed in different solvents, while Figure 5b shows the respective anisotropy decays. The dye coverage was slightly different for these samples, especially for the case of dimethoxyethane, where significant desorption of MK2 was observed. For MK2, both the transient absorption and the anisotropy decays followed similar trend, that is faster kinetics for higher Pekar factor solvents. The kinetics of both the recombination and anisotropy decays for the other carbazole dyes tested, MK147, MK3 and MK75 revealed less dependence on solvent and generally slower anisotropy decays than MK2, as shown in section 8 and 9 of the Supporting Information.

We then investigated the effect of inert ions and of the additive tert-butyl pyridine on the electron hole recombination in MK2 sensitized TiO_2 mesoporous films. Figure 5c and e illustrate that, while the addition of lithium accelerates such reaction, the addition of tBP slows it down, consistent with previous discussion by Haque et al.[38] The graphs on the right column show that the effect of tBP on recombination correlates with its effect on hole hopping, while for the case of lithium salts we do not observe any obvious correlation. The correlation is also not clear for MK147 sensitized samples in the presence of either lithium or tBP (Figure S14). For MK2, both the recombination and the anisotropy traces show decrease in dispersion upon the addition of lithium ions. Figure S16 shows that this effect is still visible for the case where a redox couple is introduced in the electrolyte. We finally compare the behaviour of samples containing either lithium or tetrabutylammonium based salts, the latter having larger size than lithium ion. We look at this comparison for the case of high and low dye coverage samples to control the ability of these cations to access the TiO_2 surface. Figure 5g and h show that, under high dye coverage conditions, LiP results in faster recombination while such effect is not there for TBAP. With low dye coverage conditions, faster recombination kinetics is instead observed for both samples where either Li or TBA salts were added.

The data in Figure 5 (and Figure S14) are summarized in Figure 6, where the hole transport $t_{r=0.1}$ and electron-hole lifetimes are plotted against the solvents' Pekar factor (6a) or against each other (6b). The resulting trends are discussed further below.

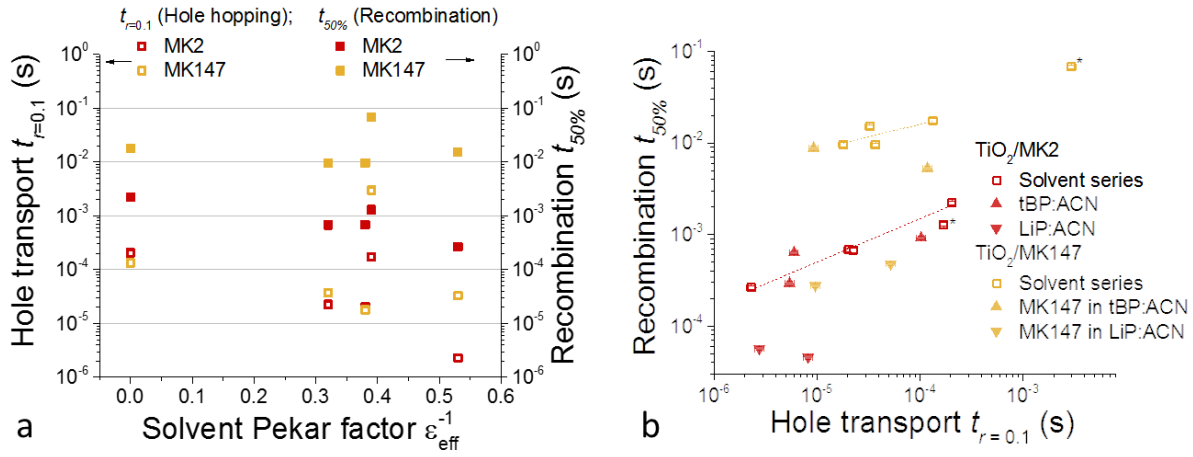


Figure 6. (a) Anisotropy and recombination kinetics as a function of the solvents' Pekar factor. (b) Correlation between rates of hole hopping and recombination for MK2 and MK147 samples measured in different solvent and inert electrolyte conditions. The dashed lines are fits to the data referred to samples immersed in solvents without additives or salts (empty symbols), omitting the measurement in DME (indicated with an '*') due to its very different value of dye surface coverage.

(iii) Dye regeneration

We finally considered MK2 or MK147 sensitized TiO_2 samples containing a redox couple in the electrolyte and measured their transient absorption spectroscopy. Figure 7 displays the oxidized dye lifetime in samples containing different concentrations of the cobalt redox couple in electrolytes based on three different solvents with Pekar factor between 0.38 and 0.53 (the transient absorption measurements are displayed in Figure S17). We note that the MK2 samples in neat solvent, for the case of dichloromethane and dimethoxyethane, showed some dye desorption. The desorption was less pronounced for the samples containing the redox couple. For the case of MK2 in acetonitrile, the transient absorption profile showed slower kinetics with rather than without the redox couple. This is a counter intuitive observation, which is due to a deceleration in electron hole recombination upon addition of the redox couple in the electrolyte compared to the case of neat solvent. We discuss this effect and a possible explanation in section 10 of the SI.

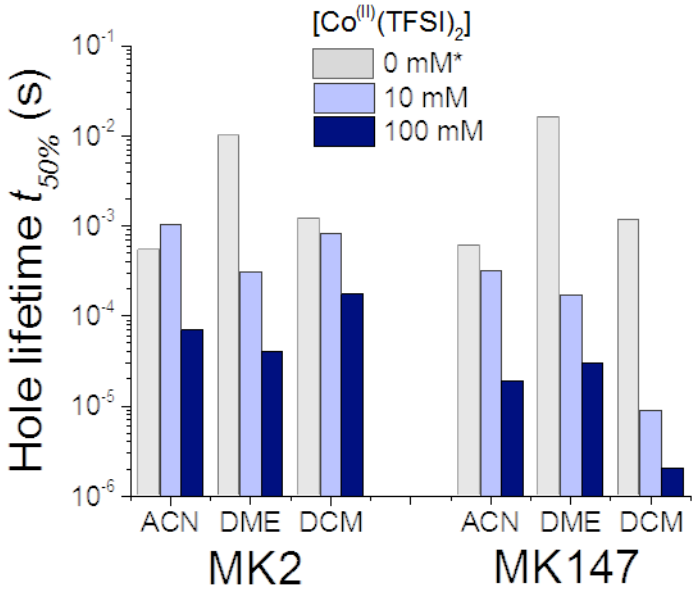


Figure 7. Hole lifetime extracted from transient absorption spectroscopy measurements on MK2 or MK147 sensitized solar cells using TiO_2 as mesoporous oxide and electrolytes containing a $Co^{(II/III)}(bpy)_3[TFSI^-]_{2/3}$ redox couple dissolved in different solvents. There was no supporting electrolyte in the solutions. The values of $t_{50\%}$ were calculated from fitting a stretched exponential function $\Delta OD = A \exp\left(-\frac{t}{\tau}\right)^{\alpha}$ to the transient absorption traces and calculating $t_{50\%} = \tau(ln2)^{1/\alpha}$ for the two dyes, the three solvents and both redox couple concentrations considered here. The data corresponding to 0 mM concentration of redox-couple (*) correspond to estimate of electron-hole recombination lifetime. For these measurements, incomplete decay was observed using a repetition rate of 5 Hz, implying that the displayed values underestimate the actual lifetime. The data referring to measurements in solvents containing the cobalt redox couple are used as estimate of the dye regeneration time.

We observed that for the 10 mM $Co^{(II)}$ case, the low Pekar factor solvents dichloromethane and dimethoxyethane showed faster reduction kinetics than acetonitrile, as expected according to Marcus theory. For the electrolyte containing 100 mM $Co^{(II)}$, DME and DCM still gave the fastest reduction kinetics for MK2 and MK147 respectively, but the half life time decreased more significantly for acetonitrile than for the other two solvents when increasing the redox couple concentration by a factor of 10. The ratio between the half-life times for the 10 mM and the 100 mM $Co^{(II)}$ is about 15 for acetonitrile, while it is between 5 and 8 for dimethoxyethane and about 5 for dichloromethane. Also, we note that while acetonitrile and dimethoxyethane gave similar results for the two dyes, the use of dichloromethane resulted in much faster kinetics of regeneration for MK147 than for MK2. This suggests that factors other than the Pekar factor determine the charge transfer rate under these

conditions. Qualitatively similar trends were observed for MK3 and MK75 (see section 8 of the Supporting Information).

As shown in Figure S17, the resistivity of the electrolytes using dichloromethane or dimethoxyethane is higher than for the case of acetonitrile at high cobalt complex concentration. In addition, the slope of the linear fit to the resistivity data as a function of solute concentration on a log-log scale is different for the case of acetonitrile and the low Pekar factor solvents (-1.2 against -0.7 to -0.9 respectively). This correlates with the slope obtained for the data of the half life times (about -1.2 for acetonitrile, -0.6 to -0.9 for dichloromethane dimethoxyethane). The case of low dye coverage of MK2:DCA sensitized TiO_2 for acetonitrile electrolytes was also considered (see Figure S18). Under this condition, where we expect negligible hole migration on the surface of the TiO_2, we observed very long lifetimes for the photogenerated hole (approaching one second) in absence of redox couple. These data show that the dependence of the regeneration rate on the redox couple concentration is not affected by the dye surface coverage. They also show that an overall faster regeneration rate than for the case of high dye surface coverage, consistent with previous reports,[39] is observed for low dye surface coverage.

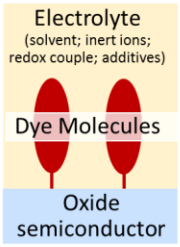
Next, we investigated the effect of inert salts in acetonitrile on the kinetics of regeneration. In section 13 of the Supporting Information, we compare the regeneration process in solar cells with different concentrations of the redox couple and lithium based inert salt. At high redox-couple concentrations, we observe faster regeneration kinetics when inert ions are added to the electrolyte. For the case of 10 mM concentration only the dynamics of the decay are slightly varied yielding a less dispersive profile, implying Li cations increase the homogeneity of the potential profile at the vicinity of the TiO_2 surface. In addition, we could expect that adsorption of lithium ions on the TiO_2 surface would attract anions at the interface between dye layer and electrolyte, which in turn would favor the approach of positively charged cobalt complexes. To further explore the hypothesis, we performed measurements of dye regeneration for electrolytes where the total concentration of inert salt is constant and where we vary the relative amount of lithium and TBA cations in solution (see Figure S19c and d). In this way, we could assess the effect of the cation size by keeping similar ionic strength of the electrolyte and any change in dielectric environment due to the inert ionic species. While adding TBAP in the electrolyte led to faster regeneration rates compared to the sample without inert ions, the increase in regeneration rate was larger for the case of lithium by a factor of about 2 to 3 than for the electrolytes with TBA cations.

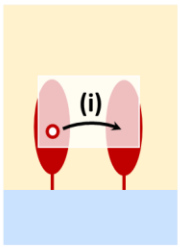
These results show that low Pekar factor solvents result in fast regeneration at low redox-couple concentrations. At redox-couple concentrations that are relevant to solar cell applications however, fast regeneration can be achieved with polar solvents that reduce ion-pairing in the electrolyte and addition of appropriate inert ions that modify the surface properties of the dye/oxide surface.

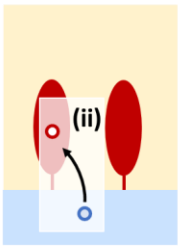
Discussion

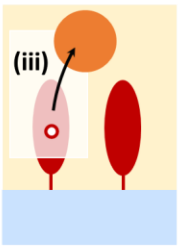
We summarize the observations from this work in Table 2 where we show the observed dependence of the three hole transfer processes investigated against each parameter of the molecular sensitized oxide systems considered in this study. Below we discuss these observations in detail.

Table 2. Summary of the observed effects on the three electron transfer processes occurring at the interface of molecular sensitized oxides in an electrolyte investigated in this study when varying experimental parameters. An up arrow indicates an increase, a down arrow indicates a decrease, and a tilde (~) indicates approximately no change. To each observation, we also add the interpretation proposed in this study. Unless specified, the results refer to acetonitrile based electrolyte and MK2/TiO_2, deviations in behavior were observed depending on the dye structure.









Variable	Hole transport rate	Recombination rate	Regeneration rate
↑ **Solvent Pekar factor**	↑ Dye dependent No correlation with measured E_{act}	↑ Possibly due to ↑ hole hopping	↓ Marcus normal region
↓ **Dye solubility in solvent**	↑ Change in E_{act} and J	↑ Possibly due to ↑ hole hopping	↓ Decrease in dye cross section
↓ **Dye surface coverage**	↓↓ Percolation behavior	↓↓ Possibly due to ↓ hole hopping	↑ Increase in dye cross section
↑ **[Li salts]**	~ ↑ E_{act} ↓ Energetic disorder	↑ ↓ Dispersion, Access to oxide surface	↑ Change in double layer properties
↑ **[TBA salts]**	~ Slight ↑ E_{act}	↑ Access to oxide surface (only at low dye coverage)	↑ Change in double layer properties
↑ **[tBP additive]**	↓ Decrease in electronic coupling between dyes	↓ Possibly due to ↓ hole hopping	

Hole hopping between dyes. The activation energies for hole hopping between dyes obtained from our measurements are in the order of 200 to 400 meV. This range corresponds to values of about 800 to 1600 meV for the reorganization energy, consistent with previous results based on electrochemical measurements.[25,40] One key observation is that no clear trend is present between the value of activation energy and the dielectric properties of the solvent. Only the TiO_2/MK2/oDCB samples can give significantly higher activation energy, opposite to what is expected given the relatively low Pekar

factor of this solvent. Another observation is that the activation energy tends to increase with time during the hole hopping process regardless of the oxide material and of the solvent used.

In our previous study, we reported that Monte Carlo simulations of hole hopping between dyes affected by energetic disorder with σ_E of about 100 meV reproduced the dispersive behaviour of transient absorption anisotropy measurements for D131 sensitized TiO_2 films.[8] We also suggested that energetic disorder was responsible for the overestimation of reorganization energy obtained with temperature dependent cyclic voltammetry compared to DFT simulations of the same parameter. Here, based on our simulations of hole hopping in disordered and disorder-free systems presented in Figure 4d, we argue that energetic disorder is likely to be the dominant contribution to the observed (increasing) hopping distance dependent activation energy. This is also consistent with values of energetic disorder that were suggested in a previous study to explain the dependence of the regeneration yield in DSSCs on the driving force of this reaction.[41] We therefore interpret the increase in activation energy shown in Figure 3d and 4 in terms of holes statistically following an energetically "downhill" diffusion path. As holes diffuse to more energetically stable sites, the activation energy for hopping and the waiting time between hopping events gradually increase, also consistent with the dispersive character of the transient absorption anisotropy data. The data presented in Figure 3a show that not only the absolute value of E_{act} is similar for samples using different solvents and oxides, but also that there is no clear trend between the slope of E_{act} with respect to the anisotropy change (% r_{exp} decay) and the dielectric environment. This suggests that similar energetic disorder is affecting hole hopping under this set of conditions.

The use of both LiP:ACN and TBAP:ACN electrolytes resulted in higher values for the activation energy compared to neat solvent. The case of lithium salt showed negligible changes in activation energy as a function of change in r_{exp}, which implies a lower energetic disorder in the dye monolayer. This is also supported by less stretched anisotropy decays for samples with Li salts in the electrolyte. Given the ability of lithium to adsorb on the TiO_2 surface, as opposed to the larger size TBA ions, this would suggest that small ions can be used to reduce the energetic disorder originating from the TiO_2, and to increase the activation energy of hole hopping. The similar increase of activation energy as a function of distance travelled by the holes that we observed for various conditions also suggests that energetic disorder is not screened by the solvent, regardless of its polarity. For the case of tBP, a negative activation energy was extracted at early time scales. This suggests 'depolarization' of the photogenerated hole occurs more favourably at low temperatures for this sample. One possible explanation could be that tBP is included in the dye layer at room temperature, causing a decrease in hole hopping rate. The 'solubility' of tBP molecules in the dye layer might be lower at low temperatures, no longer obstructing hole transfer between dyes. As a result, under these circumstances and at least for the first charge transfer steps, the anisotropy decay would appear faster at low temperature than it does at high temperatures. Similar solubility arguments might explain the low

anisotropy values measured at early timescales and low temperature for other samples (see Figure S9–S10).

The fact that similar activation energies are extracted for very different dielectric constant environments is a striking observation, which implies that the solvent reorganization energy is not a rate determining parameter under these conditions. Similar activation energies are extracted for the case of MK2 sensitized SnO_2 or TiO_2 confirming previous predictions of limited contribution of the substrate on the reorganization energy of hole transfer between dyes.[42] One possibility for the absence of solvent dependence is that the reorganization energy here could be largely influenced by neighboring dyes and/or by the extent to which solvent molecules can penetrate the dye layer. As a consequence, the contributions of all components, including the dye layer[43] and 'solvating' solvent molecules, should be considered to quantify the variations in the relevant dielectric properties of the system under different conditions. This might be particularly important for the large dyes used here, since the neighboring molecules may make the dominant contribution to the surrounding environment's dielectric properties. In Figure S21 of the Supporting Information, we show comparisons of solubility of the MK2 and MK147 dyes in the solvents used in this work. We observed high solubility of the molecules in oDCB compared to the other solvents considered here, which could be related to the large value of activation energy extracted for this solvent. Indeed, a strong tendency to solvate the dyes is expected to increase the number of solvent molecules that penetrate the dye layer and that undergo reorientation upon hole transfer between dyes, resulting in large reorganization energy. Additionally, increasing the separation *R* between molecules undergoing electron transfer would also reduce the fraction of solvation atmosphere that is shared by two units and result in an increase of λ_0 as shown in Equation 2.[44] On the other hand, the fact that oDCB is a relatively big molecule could affect its ability to penetrate the dye layer and potentially underlie the sample to sample variation observed for the activation energy measurements of samples using this solvent (Figure S8).

Besides the reorganization energy, differences in dye-solvent interactions are expected to influence the electronic coupling between dyes in terms of electronic orbital distribution, dye packing (dye conformation and configuration relative to other dyes and to the oxide surface) and tunnelling energy barrier.[30,45] In other words, the anisotropy decays reported here for different conditions cannot be solely related to the effect of the dielectric environment.

Electron-hole recombination. The recombination kinetics of MK2 sensitized TiO_2 films shown in Figure 5a follow a similar trend with the Pekar factor of solvents as previously reported for the MP13 dye.[8] Specifically, lower values of the Pekar factor resulted in slower recombination rates. Here we discuss the different interpretations resulting from different models for recombination. When considering an electron transport limited model, the data shown in Figure 5a would imply different

electron transport properties in the TiO_2 depending on the solvent, specifically with high polarity solvents resulting in faster transport. In the electron-hole recombination were instead limited by electron transfer at the oxide/dye interface (reaction limited), our results would suggest that recombination might be happening in the Marcus inverted region, where increase in solvent Pekar factor (and reorganization energy) increases the rate of electron transfer. In the inverted regime, faster kinetics are expected for the high polarity solvents also due to the stabilization of the charge separated state, in comparison with the recombined 'neutral' state, which results in lower values of driving force.[46,47]

Another explanation, which we previously proposed, is that the hole hopping process increases the recombination rate.[8,9] According to this model, the reaction at the interface is the rate limiting step, however an important contribution may come from hole migration on the surface, which enables the encounter of electrons and holes at 'suitable' reaction sites. The data shown in Figure 6b for the case of pure solvents show correlation between these two processes for MK2. Since we expect hole hopping to be an independent process to recombination, the data suggest that the hole hopping rates control the recombination kinetics, also consistent with the remarkably long life time achieved for MK2 at low surface coverage, where hole hopping is hindered (see Figure S18). For MK147 (see Figure S14), which has a similar HOMO level to MK2, and the other dyes tested (see Figure S13), we observed slower recombination kinetics and an overall less clear dependence of recombination on either of the solvent's Pekar factor or the hole hopping rate. The difference in behavior between MK2 and the other dyes could be due to the faster rate of hole hopping observed for MK2 compared to MK147, MK3 and MK75. We also note that all these dyes, apart from MK2, have their HOMO orbital more localized on the carbazole unit, therefore far from the TiO_2 surface, which would also contribute to decrease the recombination rate. For the data points related to MK2 in electrolytes containing tBP, recombination seems, again, to correlate with the hole hopping rate. This is consistent with the hypothesis that tBP may disrupt the monolayer configuration, thus decreasing electronic coupling between dyes and significantly slowing hole migration on the surface and the collision frequency of holes with TiO_2 electrons.

On the other hand, the increase in recombination rate observed for samples which included lithium salts does not in general correspond to a faster rate of hole hopping. The change in recombination kinetics due to inert ions is more likely to come from faster ambipolar diffusion compared to the ion-free case.[48] The effect is present also for the case of tetra-butyl ammonium based salts but only when low dye loading samples are considered. Since no major dependence on the type of ion is normally observed for the ambipolar diffusion coefficient of cells with large electrolyte concentrations,[49,50,51] this result suggests that access of the cation to the oxide surface is key to the increased recombination rate. Addition of tBP to an electrolyte containing LiP still induces a decrease in recombination rate as discussed above. This suggests that the beneficial presence of both additives in high performance

DSSCs might be related to a balanced tuning of conduction band edge potential, decrease in surface energetic disorder and increase in electron hole lifetime. Finally, we note that, for the case of SnO_2 sensitized films, the effect of tBP and lithium ions on recombination was negligible (Figure S15). This is consistent with the low tendency of lithium ions to adsorb on the surface of SnO_2 (unpublished results).

Dye regeneration. For dye regeneration, at low concentrations of the redox couple and in absence of other inert ions, we finally observed that higher electron transfer rates correlated with lower Pekar factor solvents. Since the dye regeneration occurs at the interface between adsorbed dyes and freely moving Cobalt complexes, donor moieties of the dyes and the redox-couple are exposed to solvent molecules, probably satisfying the assumptions that lie behind equation 1. At high concentrations, lower Pekar factor solvents still showed faster regeneration than acetonitrile but the increased rate did not scale with the increase of the $Co^{(II)}$ complex concentration from 10 to 100 mM. To explain this observation, we consider the change in the dielectric properties of the low Pekar factor solvents upon the addition of the redox couple. While for high dielectric constant solvents the addition of salts results in a limited increase (or even a decrease) in the static dielectric constant, low polarity solvents can show significant increase of this parameter upon addition of ionic species. For the case of low dielectric constant solvents, ion pairs increase the dielectric constant of the electrolyte, giving rise to higher effective Pekar factors with increasing ionic concentration.[52,53,54] In addition, we expect that ion pairs of cobalt complexes and counter ions may respond differently from unpaired cobalt complexes to the changes in electric field during the charge separation process, due to their larger volume and mass, and lower charge. This would result in different populations of reducing complexes which would show different dynamics on approaching and interacting with the dye layer as well as at undergoing the electron transfer reaction. Using impedance measurements on electrolyte sandwiched between platinum electrodes, we showed that the change in regeneration half life with redox couple concentration correlates with the change in resistance, suggesting that the concentration of active redox couple might be the same as the concentration of 'conductive' redox couple. This would be consistent with the above hypothesis, given that cobalt complexes that are paired with counter ions are not as efficient at carrying out the dye regeneration process as their unpaired counterparts. The implication for DSSC devices is that the design of a low Pekar factor environment in proximity of the dye layer could still be beneficial to the regeneration rate and ultimately to the device performance. However, at the redox couple concentration levels needed to support high operating current densities, a high polarity electrolyte is needed in the bulk of the pores of the mesoporous film. This could be achieved by designing a two solvent system, maybe using a gel phase for a solvent layer on the top of the dyes. Additional contributions to the difference in regeneration rates observed could be due to different levels of solvation of the dyes due to their higher solubility in dichloromethane and dimethoxyethane compared with acetonitrile. This can vary the geometrical area associated to the dye

(dye cross section) which redox-couple molecules can access from the electrolyte during the regeneration process. The same effect also results in very fast regeneration rates when decreasing the dye surface coverage (see Figure S18).

We showed that the presence of lithium ions in the electrolyte increases the rate of regeneration by a factor of about 3 with respect to the case of electrolytes without inert ions or electrolytes containing TBA based salts. Increase in the regeneration rate when increasing the concentration of lithium salt was previously observed for iodide triiodide based electrolytes, and it was interpreted with the attraction of I^- by the adsorbed Li^+ on TiO_2 surface.[55] However the same explanation cannot be directly applied in our case because of the cationic redox couples used here. As mentioned in the results section, the composition of the outer ionic layer (outside the dye layer) may have a different composition when either Li^+ or TBA^+ are present, due to their different size and ability to penetrate between the dyes. This difference is expected to favor the approach of $Co^{(II)}$ complexes in the case where lithium ions are used. The adsorption of lithium ions on the TiO_2 surface may electrostatically induce accumulation of negative charged ions outside of the dye layer, which attracts positively charged cobalt complexes. The presence of TBA^+ ions on the surface of the dye layer would have the opposite effect. In addition, the thickness of the double layer on TiO_2 surface would, in any case, be different for the two cations, changing the electric field profile of the dye layer including surrounding solvent molecules and Co complex concentration near the dye molecules. An additional explanation for the increase in regeneration rate may result from the presence of lithium on the surface of the TiO_2 distorting the hole molecular orbital and electron density distribution towards the dye electrolyte interface, potentially increasing the electronic coupling with colliding redox couples. While this would also decrease the coupling to electron in TiO_2, thus leading to slower recombination, the change in driving force upon addition of lithium may have a dominant effect that causes the observed increase in the recombination rate.

Conclusions

We have analyzed a fundamental prediction of non-adiabatic Marcus theory related to the role of the dielectric environment on electron transfer rates for the case of molecular sensitized semiconductors in electrolytes, these systems being relevant to DSSCs and other photoelectrochemical devices. We considered the processes of (i) hole hopping between dyes anchored to the oxide surface in inert electrolytes, of (ii) recombination between electrons in the oxide and holes on the dye, and (iii) of dye regeneration by a redox couple. For hole hopping between dyes, we found values of activation energy, in the order of 200 to 400 meV, that showed no clear correlation with the dielectric properties of the environment. This, combined with the different rates of hole hopping observed, suggests that the electronic coupling between dyes depends on the solvent and how this ‘solvates’ the dye layer. The activation energy was also a function of the distance travelled by the holes after photogeneration,

consistent with energetic disorder controlling the rate of hole hopping between dyes. Next, we showed that the rate of electron hole recombination scaled with hole hopping rates when considering different solvents, and also when including the additive tBP in the electrolyte, which slowed down both processes. We found that inert salts in the electrolyte increase the rate of recombination when the cations are able to penetrate the dye layer compared to the salt-free electrolyte case, and interpreted this effect in terms of increased ambipolar diffusion coefficient. We showed that dye regeneration by Cobalt complexes is the only process among the ones considered which roughly followed Marcus theory, probably because the redox sites are, for this reaction, largely exposed to the solvent molecules. While this observation implies that regeneration of photo-oxidized dyes in a solar cell could benefit from a low Pekar factor environment, a high polarity solvent might still be necessary in the bulk of the electrolyte to enable conductivities suitable for standard operating conditions.

Our findings imply that, for the case of systems where the distance between donor and acceptor is rather fixed, solvent effects on the reorganization energy of electron transfer might be limited and changes in the electronic coupling may dominate the charge transfer rate. Also, kinetic trends were different among the four molecules investigated, showing that interaction between dye molecules and solvent depends on the dye structure. For DSSCs, these observations suggest strategies to better control and test some widely adopted approaches to optimize device performance. Our study elucidates important consequences related to the use of inert coadsorbants within the dye layer, of lithium based inert ions, of the tert-butyl pyridine additive and of high polarity solvent based electrolytes, these being materials of choice in DSSC research. It also stresses the importance of the electrolyte composition to control the solvation of dyes, to vary the coupling between the electrochemically active components and to control the energetics and the electron transfer kinetics at the device interfaces.

Supporting Information

Experimental method; Synthesis of MK147; Notes on evaluation of activation energy from temperature dependent transient absorption anisotropy; Monte Carlo simulation of transient absorption anisotropy; Protocol for temperature dependent transient absorption anisotropy measurements; Initial value of anisotropy for MK2 sensitized TiO2 films; Temperature dependent anisotropy measurements; Solvent dependent regeneration for the dyes MK3 and MK75; Electron hole recombination; Effect of redox couple and different inert cation and anion species on oxidized dye reduction kinetics; Regeneration kinetics for MK2 and MK147 sensitized TiO2 samples; Recombination and regeneration kinetics for MK2:DCA sensitized TiO2 samples; Effect of lithium ions on kinetics of regeneration; Solubility of MK2 and MK147 in different solvents.

Acknowledgements

DM is grateful to the Japan Society for the Promotion of Science (PE18726). This work was partially supported by Grant-in-Aid for Scientific Research (B) (17H03099).

References

(1) O'Regan, B.; Gratzel, M. A Low-Cost, High-Efficiency Solar-Cell Based on Dye-Sensitized Colloidal TiO_2 Films. *Nature* **1991**, *353* (6346), 737–740. https://doi.org/10.1038/353737a0.

(2) Ardo, S.; Meyer, G. J. Photodriven Heterogeneous Charge Transfer with Transition-Metal Compounds Anchored to TiO2semiconductor Surfaces. *Chem. Soc. Rev.* **2009**, *38* (1), 115–164. https://doi.org/10.1039/b804321n.

(3) Katoh, R.; Furube, A.; Barzykin, A. V.; Arakawa, H.; Tachiya, M. Kinetics and Mechanism of Electron Injection and Charge Recombination in Dye-Sensitized Nanocrystalline Semiconductors. *Coord. Chem. Rev.* **2004**, *248*, 1195–1213. https://doi.org/10.1016/j.ccr.2004.03.017.

(4) Tachibana, Y.; Haque, S. A.; Mercer, I. P.; Moser, J. E.; Klug, D. R.; Durrant, J. R. Modulation of the Rate of Electron Injection in Dye-Sensitized Nanocrystalline TiO 2 Films by Externally Applied Bias. *J. Phys. Chem. B* **2001**, *105*, 7424–7431.

(5) Moia, D.; Cappel, U. B.; Leijtens, T.; Li, X.; Telford, A. M.; Snaith, H. J.; O'Regan, B. C.; Nelson, J.; Barnes, P. R. F. The Role of Hole Transport between Dyes in Solid-State Dye-Sensitized Solar Cells. *J. Phys. Chem. C* **2015**, *119* (33), 18975–18985. https://doi.org/10.1021/acs.jpcc.5b05222.

(6) Moia, D.; Leijtens, T.; Noel, N.; Snaith, H. J.; Nelson, J.; Barnes, P. R. F. Dye Monolayers Used as the Hole Transporting Medium in Dye-Sensitized Solar Cells. *Adv. Mater.* **2015**, *27* (39), 5889–5894. https://doi.org/10.1002/adma.201501919.

(7) Weisspfennig, C. T.; Hollman, D. J.; Menelaou, C.; Stranks, S. D.; Joyce, H. J.; Johnston, M. B.; Snaith, H. J.; Herz, L. M. Dependence of Dye Regeneration and Charge Collection on the Pore-Filling Fraction in Solid-State Dye-Sensitized Solar Cells. *Adv. Funct. Mater.* **2014**, *24* (5), 668–677. https://doi.org/10.1002/adfm.201301328.

(8) Moia, D.; Szumska, A.; Vaissier, V.; Planells, M.; Robertson, N.; O'Regan, B. C.; Nelson, J.; Barnes, P. R. F. Interdye Hole Transport Accelerates Recombination in Dye Sensitized Mesoporous Films. *J. Am. Chem. Soc.* **2016**, *138* (40), 13197–13206. https://doi.org/10.1021/jacs.6b04956.

(9) Sampaio, R. N.; Müller, A. V.; Polo, A. S.; Meyer, G. J. Correlation between Charge Recombination and Lateral Hole- Hopping Kinetics in a Series of Cis-

Ru(Phen′)(Dcb)(NCS)Ph2 Dye- Sensitized Solar Cells. *ACS Appl. Mater. Interfaces* **2017**, *9* (39), 33446–33454. https://doi.org/10.1021/acsami.7b01542.

(10) Ardo, S.; Meyer, G. J. Direct Observation of Photodriven Intermolecular Hole Transfer across TiO2 Nanocrystallites: Lateral Self-Exchange Reactions and Catalyst Oxidation. *J. Am. Chem. Soc.* **2010**, *132* (27), 9283–9285. https://doi.org/10.1021/ja1035946.

(11) Brennan, B. J.; Durrell, A. C.; Koepf, M.; Crabtree, R. H.; Brudvig, G. W. Towards Multielectron Photocatalysis: A Porphyrin Array for Lateral Hole Transfer and Capture on a Metal Oxide Surface. *Phys. Chem. Chem. Phys.* **2015**, *17*, 12728–12734. https://doi.org/10.1039/C5CP01683E.

(12) Chen, H.; Ardo, S. Direct Observation of Sequential Oxidations of a Titania-Bound Molecular Proxy Catalyst Generated through Illumination of Molecular Sensitizers. *Nat. Chem.* **2017**, *10* (1), 17–23. https://doi.org/10.1038/nchem.2892.

(13) Nelson, J.; Haque, S.; Klug, D.; Durrant, J. Trap-Limited Recombination in Dye-Sensitized Nanocrystalline Metal Oxide Electrodes. *Phys. Rev. B* **2001**, *63* (20), 1–9. https://doi.org/10.1103/PhysRevB.63.205321.

(14) Clifford, J. N.; Palomares, E.; Nazeeruddin, M. K.; Grätzel, M.; Nelson, J.; Li, X.; Long, N. J.; Durrant, J. R. Molecular Control of Recombination Dynamics in Dye-Sensitized Nanocrystalline TiO2 Films: Free Energy vs Distance Dependence. *J. Am. Chem. Soc.* **2004**, *126* (16), 5225–5233. https://doi.org/10.1021/ja039924n.

(15) Dang, X.; Hupp, J. T. Interfacial Charge-Transfer Pathways : Evidence for Marcus-Type Inverted Electron Transfer in Metal Oxide Semiconductor / Inorganic Dye Systems. *J. Am. Chem. Soc.* **1999**, *36* (121), 8399–8400.

(16) Kuciauskas, D.; Freund, M. S.; Gray, H. B.; Winkler, J. R.; Lewis, N. S. Electron Transfer Dynamics in Nanocrystalline Titanium Dioxide Solar Cells Sensitized with Ruthenium or Osmium Polypyridyl Complexes. *J. Phys. Chem. B* **2001**, No. 105, 392–403. https://doi.org/10.1021/jp002545l.

(17) Yan, S. G.; Prieskorn, J. S.; Kim, Y.; Hupp, J. T. In Search of the Inverted Region : Chromophore-Based Driving Force Dependence of Interfacial Electron Transfer Reactivity at the Nanocrystalline Titanium Dioxide Semiconductor / Solution Interface. *J. Phys. Chem. B* **2000**, *46* (104), 10871–10877.

(18) Feldt, S. M.; Lohse, P. W.; Kessler, F.; Nazeeruddin, M. K.; Grätzel, M.; Boschloo, G.; Hagfeldt, A. Regeneration and Recombination Kinetics in Cobalt Polypyridine Based Dye-Sensitized Solar Cells, Explained Using Marcus Theory. *Phys. Chem. Chem. Phys.* **2013**, *15*

(19), 7087–7097. https://doi.org/10.1039/c3cp50997d.

(19) Daeneke, T.; Mozer, A. J.; Kwon, T. H.; Duffy, N. W.; Holmes, A. B.; Bach, U.; Spiccia, L. Dye Regeneration and Charge Recombination in Dye-Sensitized Solar Cells with Ferrocene Derivatives as Redox Mediators. *Energy Environ. Sci.* **2012**, *5* (5), 7090–7099. https://doi.org/10.1039/c2ee21257a.

(20) Daeneke, T.; Mozer, A. J.; Uemura, Y.; Makuta, S.; Fekete, M.; Tachibana, Y.; Koumura, N.; Bach, U.; Spiccia, L. Dye Regeneration Kinetics in Dye-Sensitized Solar Cells. *J. Am. Chem. Soc.* **2012**, *134* (41), 16925–16928. https://doi.org/10.1021/ja3054578.

(21) Zhao, L.; Wagner, P.; Barnsley, J. E.; Clarke, T. M.; Gordon, K. C.; Mori, S.; Mozer, A. J. Enhancement of Dye Regeneration Kinetics in Dichromophoric Porphyrin-Carbazole Triphenylamine Dyes Influenced by More Exposed Radical Cation Orbitals. *Chem. Sci.* **2016**, *7* (6), 3506–3516. https://doi.org/10.1039/c6sc00429f.

(22) Marcus, R. A.; Sutin, N.; Marcus R. A. Sutin N. Electron Transfers in Chemistry and Biology. *Biochim. Biophys. Acta.* 1985, pp 265–322. https://doi.org/10.1016/0304-4173(85)90014-X.

(23) Cannon, R. D. Solvent Effects on Intervalence Charge Transfer. *Chem. Phys. Lett.* **1977**, *49* (2), 299–304. https://doi.org/10.1016/0009-2614(77)80592-7.

(24) Miyashita, M.; Sunahara, K.; Nishikawa, T.; Uemura, Y.; Koumura, N.; Hara, K.; Mori, A.; Abe, T.; Suzuki, E.; Mori, S. Dye-Sensitized Solar Cells : Combined Effects of Molecular Structure of Dyes and Electrolytes. *J. Am. Chem. Soc.* **2008**, *130* (14), 17874–17881.

(25) Moia, D.; Vaissier, V.; López-Duarte, I.; Torres, T.; Nazeeruddin, M. K.; O'Regan, B. C.; Nelson, J.; Barnes, P. R. F. The Reorganization Energy of Intermolecular Hole Hopping between Dyes Anchored to Surfaces. *Chem. Sci.* **2014**, *5* (1), 281–290. https://doi.org/10.1039/c3sc52359d.

(26) Vaissier, V.; Barnes, P.; Kirkpatrick, J.; Nelson, J. Influence of Polar Medium on the Reorganization Energy of Charge Transfer between Dyes in a Dye Sensitized Film. *Phys. Chem. Chem. Phys.* **2013**, *15* (13), 4804–4814. https://doi.org/10.1039/c3cp44562c.

(27) Bonhôte, P.; Gogniat, E.; Tingry, S.; Barbé, C.; Vlachopoulos, N.; Lenzmann, F.; Comte, P.; Grätzel, M. Efficient Lateral Electron Transport inside a Monolayer of Aromatic Amines Anchored on Nanocrystalline Metal Oxide Films. *J. Phys. Chem. B* **1998**, *102* (9), 1498–1507. https://doi.org/10.1021/jp972890j.

(28) Papageorgiou, N.; Grätzel, M.; Enger, O.; Bonifazi, D.; Diederich, F. Lateral Electron Transport inside a Monolayer of Derivatized Fullerenes Anchored on Nanocrystalline Metal

Oxide Films. *J. Phys. Chem. B* **2002**, *106*, 3813–3822.

(29) Wang, P.; Anderko, A. Computation of Dielectric Constants of Solvent Mixtures and Electrolyte Solutions. *Fluid Phase Equilib.* **2001**, *186* (1–2), 103–122. https://doi.org/10.1016/S0378-3812(01)00507-6.

(30) Read, I.; Napper, a.; Kaplan, R.; Zimmt, M. B.; Waldeck, D. H. Solvent-Mediated Electronic Coupling: The Role of Solvent Placement. *J. Am. Chem. Soc.* **1999**, *121* (47), 10976–10986. https://doi.org/10.1021/ja992281k.

(31) Katoh, R.; Furube, A.; Mori, S.; Miyashita, M.; Sunahara, K.; Koumura, N.; Hara, K. Highly Stable Sensitizer Dyes for Dye-Sensitized Solar Cells: Role of the Oligothiophene Moiety. *Energy Environ. Sci.* **2009**, *2* (5), 542–546. https://doi.org/10.1039/b900372j.

(32) Kajiyama, S.; Uemura, Y.; Miura, H.; Hara, K.; Koumura, N. Organic Dyes with Oligo-n-Hexylthiophene for Dye-Sensitized Solar Cells: Relation between Chemical Structure of Donor and Photovoltaic Performance. *Dye. Pigment.* **2012**, *92* (3), 1250–1256. https://doi.org/10.1016/j.dyepig.2011.08.016.

(33) Koumura, N.; Wang, Z.-S.; Mori, S.; Miyashita, M.; Suzuki, E.; Hara, K. Alkyl-Functionalized Organic Dyes for Efficient Molecular Photovoltaics. *J. Am. Chem. Soc.* **2006**, *128* (44), 14256–14257. https://doi.org/10.1021/ja0645640.

(34) *CRC Handbook of Chemistry and Physics*; Lide, D. R., Ed.; CRC Press, Boca Raton, FL, 2005.

(35) *Optical Constants · Refractive Indices of Pure Liquids and Binary Liquid Mixtures (Supplement to III/38). Group III Condensed Matter, Volume 47*; Lechner, M. D., Ed.; 2008. https://doi.org/10.1007/978-3-540-75291-2.

(36) Schott, S.; Steinbacher, A.; Buback, J.; Nuernberger, P.; Brixner, T. Generalized Magic Angle for Time-Resolved Spectroscopy with Laser Pulses of Arbitrary Ellipticity. *J. Phys. B At. Mol. Opt. Phys.* **2014**, *47* (12). https://doi.org/10.1088/0953-4075/47/12/124014.

(37) Mosconi, E.; Moia, D.; Pastore, M.; Frost, J. M.; Angelis, F. De; Barnes, P. R. F.; Nelson, J. Effect of Molecular Fluctuations on Hole Diffusion within Dye Monolayers. *Chem. Mater.* **2014**, *26*, 4731–4740. https://doi.org/10.1021/cm502629c.

(38) Haque, S. a; Palomares, E.; Cho, B. M.; Green, A. N. M.; Hirata, N.; Klug, D. R.; Durrant, J. R. Charge Separation versus Recombination in Dye-Sensitized Nanocrystalline Solar Cells: The Minimization of Kinetic Redundancy. *J. Am. Chem. Soc.* **2005**, *127* (10), 3456–3462. https://doi.org/10.1021/ja0460357.

(39) Ogawa, J.; Koumura, N.; Hara, K.; Mori, S. Deceleration of Dye Cation Reduction Kinetics by Adding Alkyl Chains to the π-Conjugated Linker of Dye Molecules. *Jpn. J. Appl. Phys.* **2014**, *53* (12). https://doi.org/10.7567/JJAP.53.127301.

(40) DiMarco, B. N.; Motley, T. C.; Balok, R. S.; Li, G.; Siegler, M. A.; O'Donnell, R. M.; Hu, K.; Meyer, G. J. A Distance Dependence to Lateral Self-Exchange across Nanocrystalline TiO_2. A Comparative Study of Three Homologous $Ru^{III/II}$ Polypyridyl Compounds. *J. Phys. Chem. C* **2016**, *120* (26), 14226–14235. https://doi.org/10.1021/acs.jpcc.6b04438.

(41) Haque, S. a; Park, T.; Holmes, A. B.; Durrant, J. R. Transient Optical Studies of Interfacial Energetic Disorder at Nanostructured Dye-Sensitised Inorganic/Organic Semiconductor Heterojunctions. *Chemphyschem* **2003**, *4* (1), 89–93. https://doi.org/10.1002/cphc.200390014.

(42) Manke, F.; Frost, J. M.; Vaissier, V.; Nelson, J.; Barnes, P. R. F. Influence of a Nearby Substrate on the Reorganization Energy of Hole Exchange between Dye Molecules. *Phys. Chem. Chem. Phys.* **2015**, *17* (11), 7345–7354. https://doi.org/10.1039/C4CP06078D.

(43) Vaissier, V.; Frost, J. M.; Barnes, P. R. F.; Nelson, J. Influence of Intermolecular Interactions on the Reorganization Energy of Charge Transfer between Surface-Attached Dye Molecules. *J. Phys. Chem. C* **2015**, *119*, 24337–24341. https://doi.org/10.1021/acs.jpcc.5b09739.

(44) Marcus, R. A. On the Theory of Oxidation-Reduction Reactions Involving Electron Transfer. I. *J. Chem. Phys.* **1956**, *24* (5), 966–978. https://doi.org/10.1063/1.1742723.

(45) Shibaev, P. V; Schaumburg, K.; Bjornholm, T.; Norgaard, K. Conformation of Polythiophene Derivatives in Solution. *Synth. Met.* **1998**, *97*, 97–104.

(46) Striplin, D. R.; Reece, S. Y.; Mccafferty, D. G.; Wall, C. G.; Friesen, D. A.; Erickson, B. W.; Meyer, T. J.; Da, V.; Carolina, N.; Uni, V.; et al. Solvent Dependence of Intramolecular Electron Transfer in a Helical Oligoproline Assembly. *J. Am. Chem. Soc.* **2004**, *126* (16), 5282–5291. https://doi.org/10.1021/ja0304289.

(47) Niemczyk, M. P.; Wasielewski, M. R. Photoinduced Electron Transfer in the Solid State : Rate vs Free Energy Dependence in Fixed-Distance Porphyrin-Acceptor Molecules Energy Scale Can Be Calibrated to Yield AGa in the Rigid. *J. Am. Chem. Soc.* **1991**, *113* (2), 719–721. https://doi.org/10.1021/ja00002a076.

(48) Kopidakis, N.; Schiff, E. A.; Park, N. G.; Van De Lagemaat, J.; Frank, A. J. Ambipolar Diffusion of Photocarriers in Electrolyte-Filled, Nanoporous TiO2. *J. Phys. Chem. B* **2000**, *104* (16), 3930–3936. https://doi.org/10.1021/jp9936603.

(49) Nakade, S.; Kanzaki, T.; Kubo, W.; Kitamura, T.; Wada, Y.; Yanagida, S. Role of Electrolytes

on Charge Recombination in Dye-Sensitized TiO 2 Solar Cell (1): The Case of Solar Cells Using the I -/I3- Redox Couple. *J. Phys. Chem. B* **2005**, *109* (8), 3480–3487. https://doi.org/10.1021/jp0460036.

(50) Goṇalves, A. D. S.; Davolos, M. R.; Masaki, N.; Yanagida, S.; Mori, S.; Nogueira, A. F. Stepped Light-Induced Transient Measurements of Photocurrent and Voltage in Dye-Sensitized Solar Cells Based on ZnO and ZnO:Ga. *J. Appl. Phys.* **2009**, *106* (6), 10803–10807. https://doi.org/10.1063/1.3226073.

(51) Wang, H.; Peter, L. M. Influence of Electrolyte Cations on Electron Transport and Electron Transfer in Dye-Sensitized Solar Cells. *J. Phys. Chem. C* **2012**, *116* (19), 10468–10475. https://doi.org/10.1021/jp211807w.

(52) Hubbard, J. B.; Colonomos, P.; Wolynes, P. G. Molecular Theory of Solvated Ion Dynamics. III. the Kinetic Dielectric Decrement. *J. Chem. Phys.* **1979**, *71* (6), 2652–2661. https://doi.org/10.1063/1.438622.

(53) Kraus, B. C. A.; Fuoss, R. M. Properties of Electrolytic Solutions. I. Conductance as Influenced by the Dielectric Constant of the Solvent Medium. *J. Am. Chem. Soc.* **1933**, *55*, 21–36. https://doi.org/10.1021/ja01328a003.

(54) Constant, T. D.; Electrolyte, B. Properties of Electrolytic Solutions. III. The Dissociation Constant. *J. Am. Chem. Soc.* **1933**, *55*, 1019–1028. https://doi.org/10.1021/ja01330a023.

(55) Pelet, S.; Moser, J.-E.; Grätzel, M. Cooperative Effect of Adsorbed Cations and Iodide on the Interception of Back Electron Transfer in the Dye Sensitization of Nanocrystalline TiO_2. *J. Phys. Chem. B* **2000**, *104* (8), 1791–1795. https://doi.org/10.1021/jp9934477.

Table of Content

